THE NUCLEAR DEFORMATION PARAMETERS AT HIGH EXCITATION ENERGIES ☆

J.L. EGIDO [1], C. DORSO [2], J.O. RASMUSSEN

Nuclear Science Division, Lawrence Berkeley Laboratory, University of California, Berkeley, CA 94720, USA

and

P. RING

Physik-Department der Technischen Universität München, D-8046 Garching, Fed. Rep. Germany

Received 8 May 1986

The behavior of the deformation parameters with increasing excitation energy is analyzed in different theories. Realistic calculations are done for the nucleus ^{158}Er. The inclusion of fluctuations leads to large departures from the mean field values.

In recent years much experimental as well as theoretical effort has been devoted to understanding properties of nuclei under extreme conditions, such as high angular momentum and/or high excitation energy [1]. On the experimental side several new phenomena have been discovered. Some examples are the observed irregularities in the yrast band of a cold nucleus and the existence of giant resonances built on excited states [2]. The quasicontinuum is now the object of intensive study by several groups. The self-consistent cranking model [3] has been successfully used for the description of the yrast line of a cold heavy nucleus. For moderately higher excitation energy one still has to consider the pairing degree of freedom as well as the temperature dependence, which complicates the use of realistic forces in calculations of Hartree–Fock–Bogoliubov type. Consequently only the semiclassical method of Strutinsky generalized to finite temperature and superfluid nuclei has been used [4] as an approximation.

☆ This work was supported in part by a Fulbright/MEC grant and by the Director, Office of Energy Research, Division of Nuclear Physics of the Office of High Energy and Nuclear Physics, of the US Department of Energy under Contract DE-AC03-76SF00098.

[1] Permanent address: Departamento de Fisica Teórica, Universidad Autonoma, Madrid, Spain.

[2] Permanent address: Facultad de Ciencias Exactas, Universidad de Buenos Aires, 1428 Buenos Aires, Argentina.

Recently the finite temperature Hartree–Fock–Bogoliubov (FTHFB) has been proposed [5] and solved [3] for separable forces with the Baranger–Kumar hamiltonian and configuration space. A systematic study of the deformation parameters, as a function of temperature, has also been made [6] in the FTHFB which as a mean-field theory neglects contributions stemming from departures from the mean values.

In all the above calculations no attention has been paid to the fluctuations due to the finite temperature. However, simple models [7,8], as well as realistic calculations [9], have shown that the effect of such fluctuations can be very important for quantities such as the pairing gap even at low temperature. The motivation of this work was to extend such investigations to other degrees of freedom such as the deformation parameters a_0 and a_2

$$a_0 = \beta \cos \gamma, \quad a_2 = \beta \sin \gamma, \tag{1}$$

which for a deformed nucleus are related to the experimentally observed quadrupole moments.

If one considers a_0 and a_2 as collective coordinates, it is possible to derive [10] at finite temperature a classical hamiltonian function in the adiabatic time-dependent Hartree–Fock theory given by

$$H(a_0, a_2, \dot{a}_0, \dot{a}_2) = \tfrac{1}{2} B_{00} \dot{a}_0^2 + \tfrac{1}{2} B_{22} \dot{a}_2^2 + B_{02} \dot{a}_0 \dot{a}_2 + V(a_0 a_2). \tag{2}$$

0370-2693/86/$ 03.50

$V(a_0, a_2)$ is given by the temperature-dependent mean-field energy, and the mass parameters B_{ij} are given by

$$B_{\mu\nu} = \tfrac{1}{2} \sum_{kl} \frac{q^{\mu}_{lk} q^{\nu}_{lk}}{|E_l - E_k|^3} |f_k - f_l|, \qquad (3)$$

where q^{μ} is the supermatrix [4]

$$\begin{pmatrix} Q^{11} & Q^{20} \\ -Q^{02} & -Q^{11T} \end{pmatrix},$$

corresponding to the multipole operators $r^2 Y_{20}$ or $(1/\sqrt{2})\,(r^2 Y_{22} + r^2 Y_{2-2})$. The quantities E_k are the quasiparticle energies

$$\begin{pmatrix} E_k & 0 \\ 0 & -E_k \end{pmatrix},$$

and f_k the occupation factors of the Fermi–Dirac distribution at temperature T, in matrix form

$$\begin{pmatrix} f_k & 0 \\ 0 & 1-f_k \end{pmatrix}.$$

The probability for the nucleus having the deformation a_0, a_2 is given [11,9] by

$$P(a_0, a_2) \approx [B_{00}(a_0 a_2)\, B_{22}(a_0 a_2) - B^2_{20}(a_0 a_2)]^{1/2} \times \exp[-F(a_0, a_2)/T]. \qquad (4)$$

$F(a_0, a_2)$ is the free energy obtained from $V(a_0, a_2)$, varying a_0, a_2 independently. In principle, one should also consider the pairing degree of freedom as an independent variable, but then the calculations become very time consuming, so we approximate these calculations by solving the gap equations for each point of the plane a_0, a_2 to find the self-consistent gap for this deformation. The chemical potentials λ_Z, λ_N, were adjusted to get the right particle numbers. In our calculations for the deformed nucleus ^{158}Er we use for $V(a_0, a_2)$ the pairing plus quadrupole hamiltonian of Baranger and Kumar [12], we also use their configuration space.

For each couple (a_0, a_2) we self-consistently determine the gap parameter for protons and neutrons for different temperatures. In fig. 1 contour plots of these

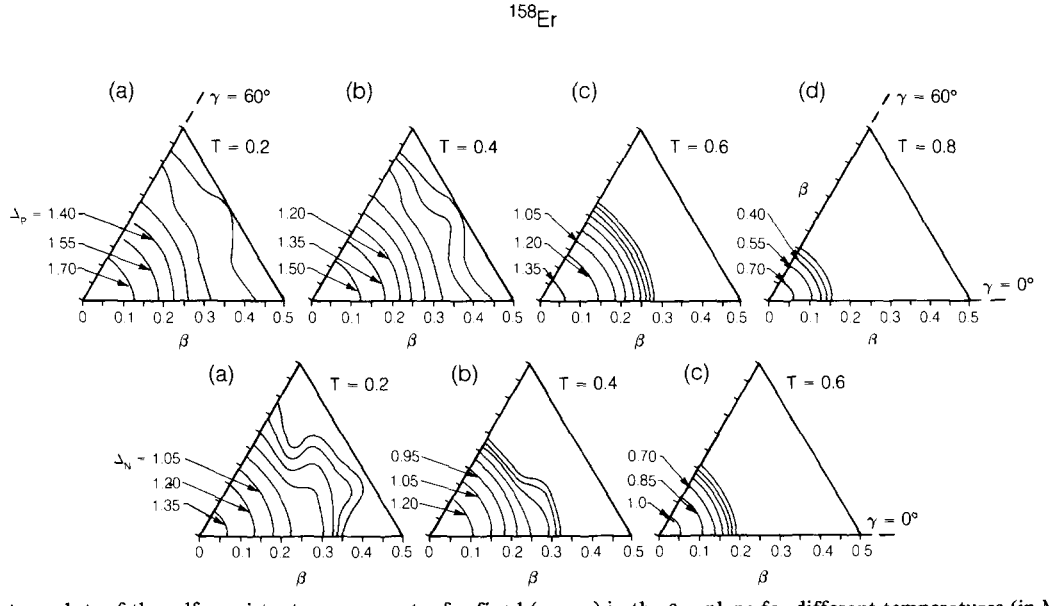

Fig. 1. Contour plots of the self-consistent gap parameter for fixed (a_0, a_2) in the β, γ plane for different temperatures (in MeV) for the nucleus ^{158}Er. In the upper part the protons gap. The contour near the origin has the value in (a) 1.7 MeV, in (b) 1.5 MeV, in (c) 1.35 MeV, and in (d) 0.7 MeV. The other contours decrease outwards with a step-size of 0.150 MeV. In the lower part the same for neutrons. The contour near the origin has the value in (a) 1.35 MeV, in (b) 1.2 MeV, in (c) 1.0 MeV. Further details as for the protons.

quantities are depicted[‡1] in the β, γ plane for protons (upper part) and neutrons (lower part). For protons at $T = 0.2$ MeV there are strong correlations in the whole β, γ plane; at $T = 0.4$ MeV they vanish only for β larger than 0.5. At $T = 0.6$ MeV they disappear for $\beta > 0.3$ and for $T = 0.8$ MeV only very weak pairing correlations remain (maximum gap is 0.7 MeV for the spherical shape) for $\beta < 0.2$. For $T > 0.8$ MeV no significant pairing was found. For the neutron gap (see the lower part of the figure) a similar trend is observed, the only difference being that the quenching of the correlations is much faster. It is interesting that the gap parameters show almost no dependence on the γ degree of freedom.

In calculating probabilities P, the mass dependence has been usually neglected [7,8] under the implicit assumption that the mass parameters do not depend strongly on the parameters involved (in our case a_0 and a_2). Only recently, in ref. [9] the probability (4) was calculated, with and without mass dependence, taking the gap parameter as a coordinate. The results for the average gap value were, qualitatively, not very different in both approximations; only a small reduction in the first calculation with respect to the second was observed.

We again would like to do both kinds of calculation for the deformation parameters. However, it is well known [13] that the cranking formula (3) has some inherent difficulties for the mass parameter in the region of a level crossing or pseudocrossing, since the denominators become very small. This difficulty increases at higher temperatures, where the gap has vanished and the particle–hole configurations give a finite contribution. In this letter it is not our intention to go beyond the approximation (3) to include further correlations which could wash out the sharpness of level crossings. On the other hand, if one wants to have some information on the effect of the mass parameter on the probability P, some kind of modification has to be done in expression (3) to avoid the possible divergences

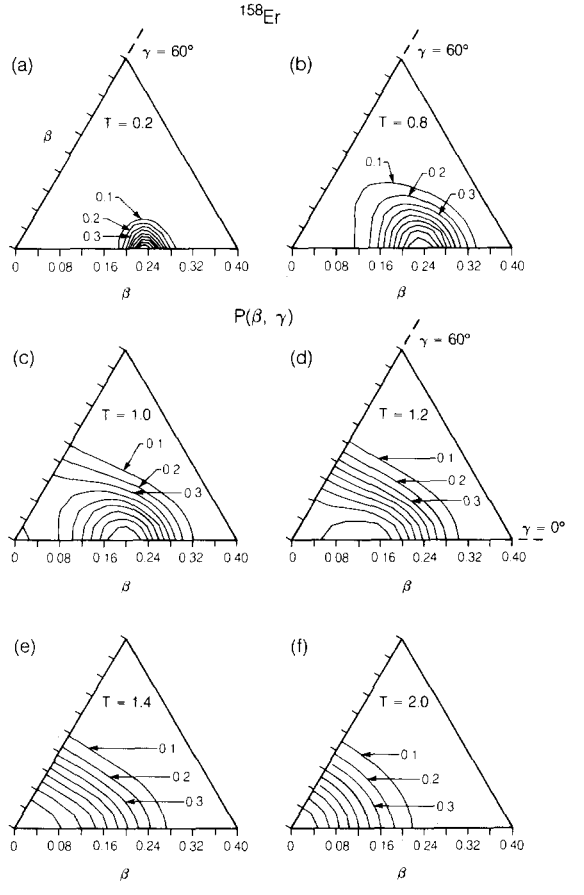

Fig. 2. The probability distribution $P(a_0, a_2)$, without mass dependence for different temperatures for the nucleus ^{158}Er. The outer contour corresponds to 0.1, it increases inwards with a step-size of 0.1, the maximum value is 1.0.

in the level crossings. We adopt the pragmatic approach of introducing a minimum level separation ϵ, stemming from the neglected residual interaction, and replace $|E_k - E_l|$ by $|E_k - E_l| + \epsilon$ in (3). We have done calculations within the range $\epsilon = 0.2$–3.0 MeV and the results are qualitatively independent of ϵ. We shall later on come back to this point. In the final results we choose $\epsilon = 1$ MeV. In the following we denote by $P(a_0, a_2)$ the probability without mass dependence and by $P_M(a_0, a_2)$ the probability with mass dependence.

In figs. 2a–2f we show the probability distribution $P(\beta, \gamma)$ without mass dependence for the nucleus ^{158}Er at zero angular momentum for the temperatures $T =$ 0.2, 0.8, 1.0, 1.2, 1.4 and 2.0 MeV. $P(\beta, \gamma)$ is normalized in such a way that the maximum value for a given

[‡1] One has to distinguish between the coordinates a_0, a_2 and $\tilde{a}_0 = \chi \langle r^2 Y_{20} \rangle$, $\tilde{a}_2 = \chi (1/\sqrt{2}) \langle r^2 (Y_{22} + Y_{2-2}) \rangle$ where χ is the strengh of the quadrupole–quadrupole interaction [12], they are equal only in the minimum. All results as well as the plots are calculated with $\tilde{a}_0$ and $\tilde{a}_2$ (in some cases the corresponding $\tilde{\beta}, \tilde{\gamma}$). We have omitted the tildes just for simpler notation.

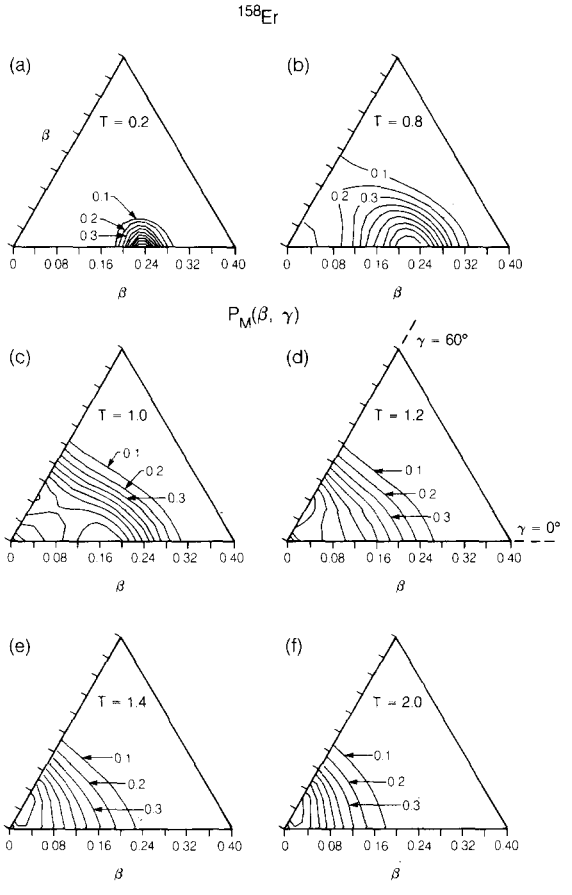

Fig. 3. The probability distribution $P_M(a_0, a_2)$, with mass dependence for different temperatures for the nucleus ^{158}Er. The outer contour corresponds to 0.1, the step-size is 0.1, the maximum value is 1.0. See text for further details.

temperature is unity. Each line in the contour plots differs by ±0.1 from the adjacent lines. For $T = 0.2$ MeV we have a strongly peaked distribution around the axially symmetric minimum at $\beta = 0.23$. At $T = 0.8$ MeV the distribution softens in all directions. At $T = 1.0$ MeV the minimum is still on the prolate side, but on the oblate side at $\beta \sim 0.1$ there is an appreciable part of the probability density. At $T = 1.2$ MeV the shifting towards the oblate side continues, while at $T = 1.4$ MeV the maximum of the distribution is already at $\beta = 0$. At $T = 2.0$ MeV the distribution is essentially that of a spherical vibrator.

The full probability distribution $P_M(a_0, a_2)$, i.e., including the mass dependence, is shown in fig. 3. For $T = 0.2$ MeV the exponential dependence in eq. (4) is too strong to be changed by the mass dependence on a_0, a_2. For $T = 0.8$ MeV we already notice some difference with respect to fig. 2, namely it softens faster toward the oblate shape. At temperature 1 MeV a second maximum appears at the oblate edge with equal probability to the prolate one. At $T = 1.2$ and 1.4 MeV the probability maximum appears for the oblate shape only. For $T = 2$ MeV the maximum extends around the spherical shape. The different behavior between

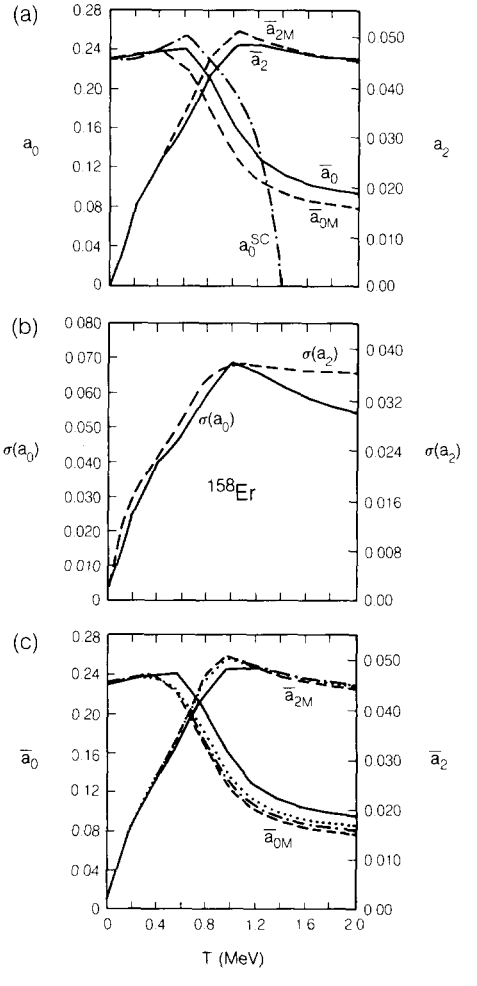

Fig. 4. In the upper part are shown the parameters a_0 and a_2 in different approximations (see text) versus the temperature. In the middle part are shown the quantities $\sigma(a_0)$, $\sigma(a_2)$. In both cases the left scale applies for a_0, whereas the right-hand one is for a_2. In the lower part of the figure the parameters $\bar{a}_{0M}$ and $\bar{a}_{2M}$ are depicted for different values of the parameter ϵ.

$P(a_0, a_2)$ and $P_M(a_0, a_2)$ can be understood classically: for an axially symmetric spheroid the irrotational mass is given [14] by $\frac{1}{5}(1+\frac{1}{2}a^2/c^2)B$, where c is the semiaxis along the symmetry axis and a the transverse. Clearly since the oblate shape has a larger mass parameter the broad distribution which appears in fig. 2 can be easily driven to the oblate shape.

In the upper part of fig. 4 we show a_0^{sc}, the self-consistent value of a_0, which corresponds to the value of a_0 in the free energy minimum in the plane a_0, a_2 for a given T. Since we are at zero angular momentum, the shape parameter γ is 0° and therefore $a_2^{sc} = 0$, ($a_0^{sc} = \beta$) for all temperatures. Also represented are the corresponding values of a_0 and a_2 but taking into account the temperature fluctuations, i.e.

$$\bar{a}_K = \langle a_K \rangle = \int a_K P(a_0 a_2)\, da_0\, da_2, \qquad K = 0, 2, \qquad (5)$$

the scale of a_0^{sc} and $\bar{a}_0$ is on the left, and that of $\bar{a}_2$ is on the right. Corresponding shape parameters $\bar{a}_{0M}$ and $\bar{a}_{2M}$ are average values calculated taking into account the mass dependence of the probability, i.e. using $P_M(a_0, a_2)$ in eq. (5).

The integration in eq. (5) runs over the area $0 \leqslant \beta < \infty$, $0 \leqslant \gamma \leqslant 60°$ in the β,γ plane. This area includes all possible quadrupole deformations and each of them is counted only once. The average values $\bar{a}_0$ and $\bar{a}_2$ have to be considered with some care. A finite $\bar{a}_2$, for example, may arise from fluctuation away from axial symmetry and not necessarily mean a most probable asymmetric shape. In order to understand the full picture, we have always to keep in mind the entire distributions as given in figs. 2 and 3. At temperatures $0 < T < 0.5$ parameter a_0^{sc} (or β) slightly rises, mainly because of the reduction of pairing correlations with growing temperature. Between $T = 0.6$ and 1.1 MeV the temperature destroys the shell effects and we observe a diminution of the deformation. For $T > 1.1$ MeV the fluctuations are so large that the mean-field approach breaks down, and the deformation drops dramatically from 0.16 at $T \sim 1.1$ MeV to zero at $T \sim 1.4$ MeV.

The average values $\bar{a}_0$ behave qualitatively in a similar manner to a_0^{sc} for temperatures $T \leqslant 1.1$ MeV, but for T larger than 1.1 MeV, $\bar{a}_0$ does not decrease but approaches the value ~ 0.10, as can be understood from the probability distribution $P(\beta, \gamma)$ in fig. 2. The parameter a_2^{sc}, as mentioned above, is always zero because of axial symmetry; $\bar{a}_2$ rises with a rather steep slope from 0 to 0.045 at $T \sim 1.1$, then remains almost constant around this value. This behavior can also be understood from fig. 2. The parameter $\bar{a}_{2M}$ is rather similar to $\bar{a}_2$ for all temperatures. The parameter $\bar{a}_{0M}$ looks like $\bar{a}_0$ for temperatures lower than 0.4 MeV but for higher temperatures exhibits smaller values due to the fact that the maximum on the oblate side has a smaller β value. In both cases the sharp collapse of the deformation is smeared out by the temperature fluctuations. The neglect of the mass dependence overemphasizes this effect.

In fig. 4b the quantities $\sigma(a_0)$ and $\sigma(a_2)$ are represented. The variance is defined by

$$\sigma^2(a_K) = \langle \bar{a}_K^2 \rangle - \langle \bar{a}_K \rangle^2, \qquad K = 0.2. \qquad (6)$$

Again the left-hand scale is for a_0 and the right-hand scale for a_2. Both of them behave in a similar way. They rise quickly from $T = 0$ MeV, to $T \sim 1.1$ MeV and then stabilize, or slightly decrease, for higher temperatures. Finally to have some feeling about the dependence of the different quantities on the parameter ϵ introduced to avoid the possible singularities of the mass parameters, we show in fig. 4c the average deformations $\bar{a}_{0M}$ and $\bar{a}_{2M}$ for some values of ϵ. The dashed lines correspond to $\epsilon = 0.5$, the dashed–dotted to $\epsilon = 1.0$ and the dotted to $\epsilon = 1.5$ MeV, the bold ones are for $\bar{a}_0$ and $\bar{a}_2$, i.e., when the mass dependence is neglected. From this figure one can conclude that the dependence on ϵ is rather smooth in a broad range. For very large values of ϵ the possible structure is washed out and we expect the limiting value of $\bar{a}_0$ and $\bar{a}_2$, respectively.

In summary, we have for the first time self-consistently taken into account the temperature fluctuation in the calculation of the deformation parameter for ^{158}Er in realistic calculations. The effects on a_0 are large for $T \geqslant 1.1$ MeV; on a_2 they become appreciable already for small temperatures.

One of the authors (J.L.E.) would like to acknowledge the Nuclear Science Division, especially R.M. Diamond and F.S. Stephens, for the hospitality extended to him during his stay at the Lawrence Berkeley Laboratory. W. Swiatecki is also thanked for a discussion.

References

[1] B. Herskind, Nuclear Structure and heavy ion dynamics, LXXVII Corso (Societa Italiana de Fisica, Bologna, Italy, 1984) p. 68.
[2] J.O. Newton, B. Herskind, R.M. Diamond, E.L. Dines, J.L. Draper, K.H. Lindenberger, C. Schuck, S. Shin and F.S. Stephens, Phys. Rev. Lett. 46 (1981) 1383.
[3] J.L. Egido and P. Ring, Nucl. Phys. A 388 (1982) 19, and references therein.
[4] P. Ring, L.M. Robledo, J.L. Egido and M. Faber, Nucl. Phys. A 419 (1984) 261, and references therein.
[5] A.L. Goodman, Nucl. Phys. A 369 (1981) 365; K. Tanabe, K. Sugawara-Tanabe and H.J. Mang, Nucl. Phys. A 357 (1981) 20, 45.
[6] J.L. Egido, P. Ring and H.J. Mang, Nucl. Phys. A 451 (1986) 77.
[7] L.G. Moretto, Phys. Lett. B 44 (1973) 494.
[8] A.L. Goodman, Phys. Rev. C 29 (1984) 1887.
[9] J.L. Egido, P. Ring, S. Iwasaki and H.J. Mang, Phys. Lett. B 154 (1985) 1.
[10] M. Baranger and M. Veneroni, Ann. Phys. (NY) 114 (1978) 123.
[11] E.M. Lifshitz and L.P. Pitaevskii, Statistical physics, Vol. 1 (Pergamon, London, 1980).
[12] M. Baranger and K. Kumar, Nucl. Phys. A 110 (1968) 490.
[13] V.M. Strutinski, Z. Phys. A 280 (1977) 99.
[14] M. Lamb, Hydrodynamics, 6th Ed. (Dover, New York, 1945).